Supplemental Data

Competitive binding between dynamic p53 transactivation subdomains to human MDM2 Protein: Implications for regulating the p53·MDM2/MDMX interaction

Bing Shan, Da-Wei Li, Lei Bruschweiler-Li, and Rafael Brüschweiler

Department of Chemistry and Biochemistry, The Florida State University, Tallahassee, Florida 32306 and National High Magnetic Field Laboratory, The Florida State University, Tallahassee, Florida, 32310

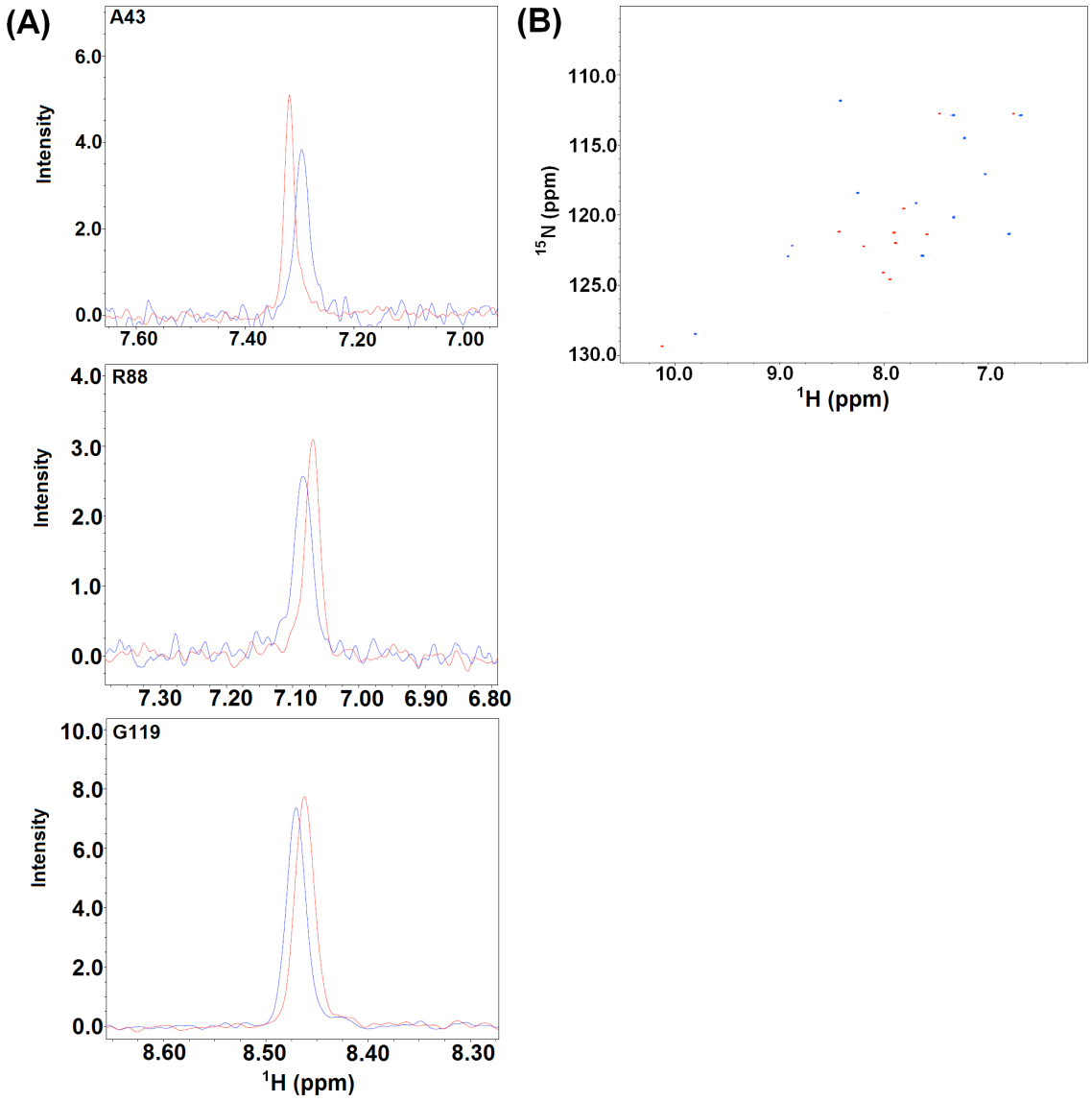

Figure S1. (A) Effect of complex formation on NMR linewidths of MDM2. Selected cross sections through ^{15}N-^{1}H HSQC cross peaks of ^{15}N-labeled apoMDM2 (red) and ^{15}N-labeled MDM2·p53TAD (blue). Peak assignments are given in the upper-left corner of each panel; (B) overlay of the ^{15}N-^{1}H HSQC spectra of apoTAD1 (red) and TAD1 ·MDM2 (blue). The concentration of ^{15}N-labeled TAD1 peptide was 250 μM in both samples. The TAD1·MDM2 complex contained 250 μM of MDM2. NMR ^{1}H,^{15}N HSQC

cross-peaks of TAD1 peptide undergo only moderate broadening upon binding to MDM2, which is in contrast to the behavior of p53TAD (Figure 2).

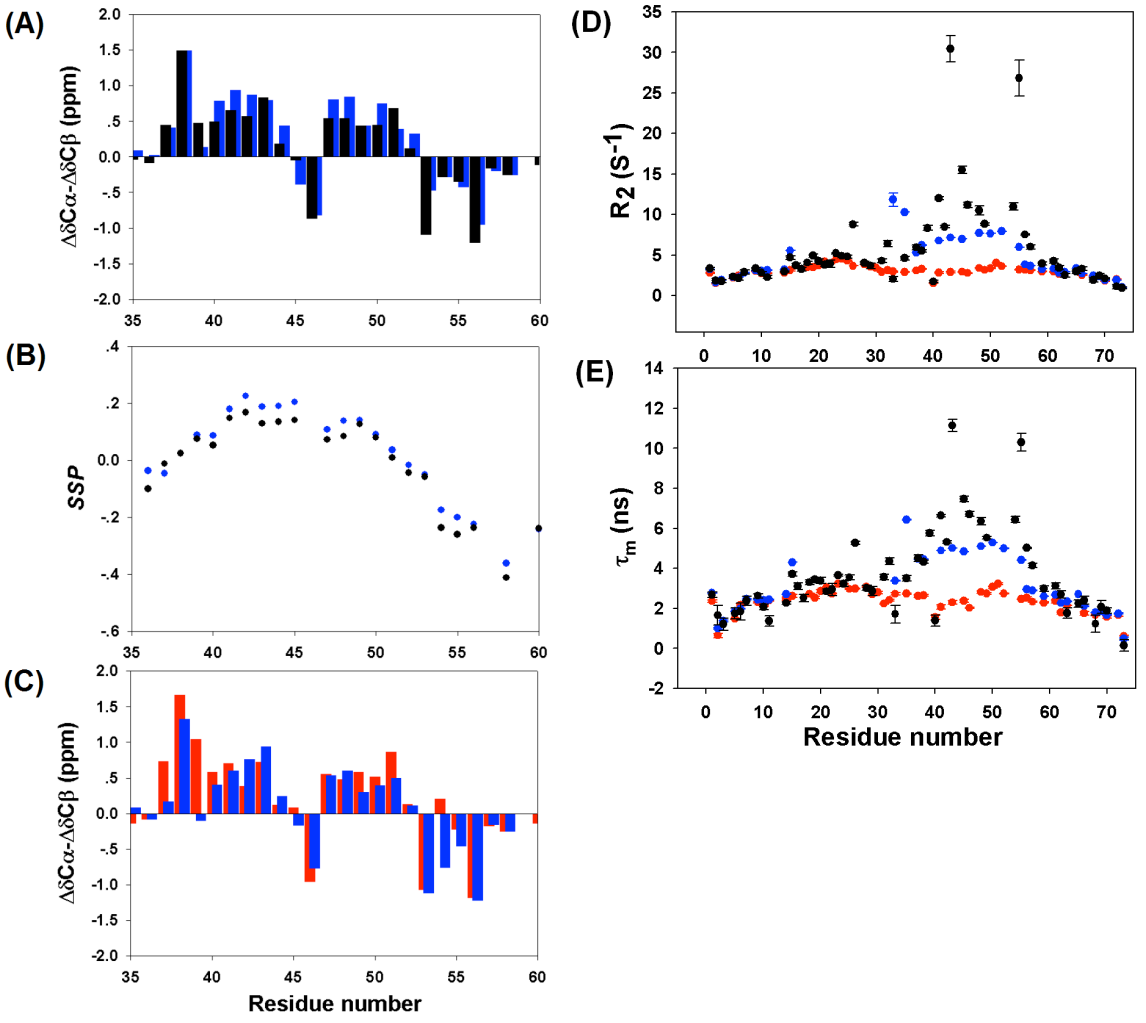

Figure S2. Structural propensities of TAD2 region of p53TAD WT and p53TAD F19A/W23A upon MDM2 binding. (A) ^{13}C $\Delta\delta C_\alpha - \Delta\delta C_\beta$ secondary shifts for the MDM2 bound state of p53TAD WT (●) and MDM2-bound state of p53TAD F19A/W23A (●). Positive numbers indicate α-helical and negative values β-strand structural propensity; (B) Secondary Structure Propensity (SSP) analysis of the MDM2 bound state of p53TAD WT (●) and MDM2-bound state of p53TAD F19A/W23A (●). Positive SSP indicates propensity to form an α-helical structure and negative SSP suggests β-strand structure. (C) $\Delta\delta C_\alpha - \Delta\delta C_\beta$ secondary shifts for apop53TAD F19A/W23A (blue bars) and p53TAD F19A/W23A·MDM2 (red bars). In (C) the secondary shifts of the MDM2-bound state were calculated by multiplying the difference of the chemical shifts between the free state

and the experimental observed bound state by a factor of 2 to take into account that only ~50% of apop53TAD F19A/W23A is bound to MDM2 while in fast exchange. (D) Backbone ^{15}N transverse (R_2) relaxation rates of apop53TAD WT (●), p53TAD WT·MDM2 (●) and p53TAD F19A/W23A·MDM2 (●); (E) Rotational correlation time estimates of apop53TAD (●), p53TAD WT·MDM2 (●) and p53TAD F19A/W23A·MDM2 (●) from the ratio of transverse and longitudinal relaxation rates of ^{15}N (R_2/R_1). The calculation was performed using the quadric diffusion program provided by Prof. Arthur G. Palmer III.

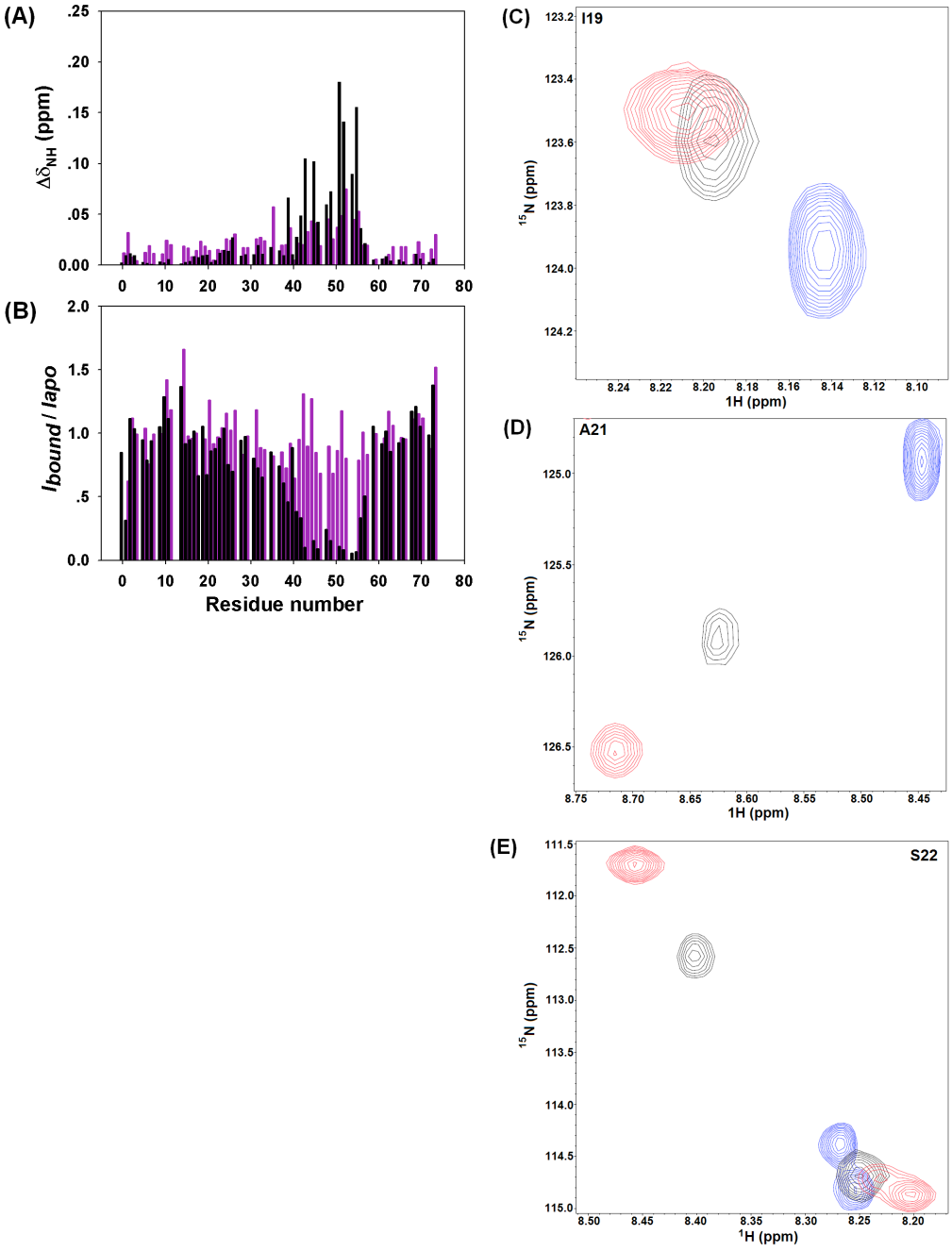

Figure S3. (A) Chemical shift perturbations of p53TAD F19A/W23A induced by MDM2 binding in the absence and presence of the drug lead nutlin-3; $\Delta\delta_{NH} = \sqrt{(\Delta\delta_{HN}{}^2 + (0.15 \times \Delta\delta_N)^2)}$. Black bars: Δδ between p53TAD F19A/W23A and p53TAD F19A/W23A·MDM2; pink bars: Δδ between p53TAD F19A/W23A and p53TAD F19A/W23A·MDM2 in the presence of 1 mM nutlin-3; (B) the calculated peak intensity

ratios (I_{bound}/I_{apo}) between p53TAD F19AW23A·MDM2 and p53TAD F19A/W23A and (●) and p53TAD F19A/W23A·MDM2 in presence of 1 mM nutlin-3 and p53TAD F19A/W23A (●); Panel C through panel E: Selected regions of $^{1}H,^{15}N$ HSQC spectra corresponding to representative lid residues I19 (C), A21 (D), and S22 (E) for apoMDM2 (red), MDM2·p53TAD F19A/W23A (black) and MDM2·p53TAD wild-type (blue). Upon interaction of MDM2 with p53TAD F19A/W23A, the cross-peaks of these three lid residues move from a state that is self-associated with the hydrophobic cleft (red) toward the cross-peaks of the open lid state of p53TAD·MDM2 (blue), reflecting that the lid conformation of MDM2·p53TAD F19A/W23A shifts to a partially open state.

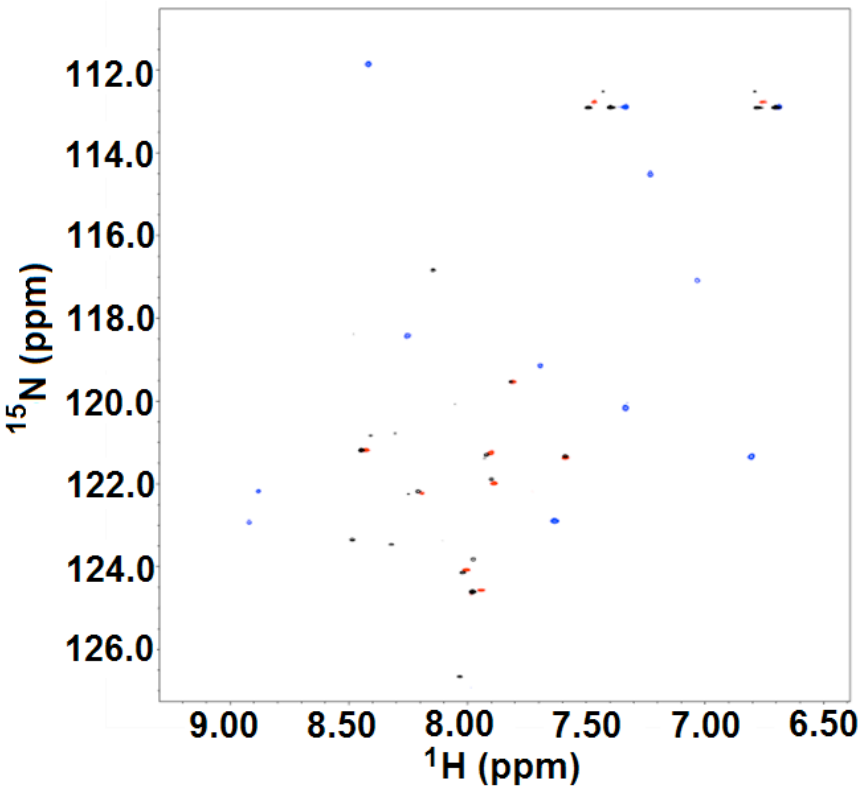

Figure S4. Further direct evidence for competitive binding between TAD2 and TAD1 to MDM2. Superimposition of the ^{15}N-^{1}H HSQC spectra of ^{15}N-labeled apoTAD1 peptide (●, red); ^{15}N-TAD1·non-labeled-MDM2 (●, blue) and ^{15}N-TAD1·non-labeled-MDM2·non-labeled-TAD2 (●, black). The concentration of ^{15}N-TAD1 peptide was 120 μM in all samples. The TAD1·MDM2 complex contained 240 μM of MDM2. The TAD1/MDM2/TAD2 mixture contained 240 μM of MDM2 and more than 2 mM TAD2 peptide. The close correspondence of the red peaks and black peaks reflects that TAD2 successfully competes with TAD1 in binding to MDM2 by suppressing the interaction between TAD1 and MDM2.

Binding polynomial analysis

The binding polynomial Q for a competitive binding mechanism between the two subdomains TAD1 and TAD2 of p53TAD to MDM2 is given by

$$Q[MDM2] = [MDM2] + [MDM2 : p53TAD_1][p53TAD] + [MDM2 : p53TAD_2][p53TAD] \tag{S1}$$

where $[MDM2]$ denotes the free MDM2 concentration, $[p53TAD]$ denotes the free p53TAD concentration, $[MDM2 : p53TAD_1]$ denotes the concentration of the MDM2·p53TAD complex with TAD1 bound to the binding pocket of MDM2, and $[MDM2 : p53TAD_2]$ denotes the concentration of the MDM2·p53TAD complex with TAD2 bound to the binding pocket of MDM2.

With the association constants K_{a1} and K_{a2} given by

$$K_{a1} = \frac{[MDM2 : p53TAD_1]}{[MDM2][p53TAD]} \quad \text{and} \quad K_{a2} = \frac{[MDM2 : p53TAD_2]}{[MDM2][p53TAD]} \tag{S2}$$

it follows for the binding polynomial Q:

$$Q = 1 + (K_{a1} + K_{a2})[p53TAD] = 1 + K_a[p53TAD] \tag{S3}$$

Conversion of the effective association constant K_a to the dissociation constant K_d yields

$$K_d = \frac{K_{d1} \cdot K_{d2}}{K_{d1} + K_{d2}} \tag{S4}$$

Eq. S4 shows that the effective dissociation constant K_d for the competitive binding event is always smaller (tighter binding) than either one of the binding constants K_{d1} and K_{d2}. Competitive binding can lower the dissociation constant of the smaller of the two binding constants by up to a factor of 2.